Acceleration and Cooling Effects in Laminar Boundary Layers—Subsonic, Transonic, and Supersonic Speeds

L. H. BACK*
Jet Propulsion Laboratory, California Institute of Technology, Pasadena, Calif.

The structure of laminar boundary layers is investigated analytically over a large range of flow acceleration, surface cooling, and flow speeds. For flow of a perfect gas over an isothermal surface, the transformed boundary-layer equations with the similarity assumption were solved numerically for values of the acceleration parameter $\bar{\beta}$ up to 20, a value not uncommon to transonic flow in supersonic nozzles, and for flat-faced bodies placed in supersonic flow, as well as for values of the surface-to-total-gas enthalpy g_w ranging from 0 (severely cooled surface) to 1. The solutions were inverted and shown in the physical plane where the velocity and total enthalpy profiles depend upon the flow speed or compressibility parameter S in addition to $\bar{\beta}$ and g_w. Friction and heat transfer parameters, as well as thicknesses associated with the boundary layer, are also shown. In general, the effects of acceleration, cooling, and flow speed are significant, but the dependence of the heat-transfer parameter on $\bar{\beta}$ and g_w is weak when g_w is small. Application of the similarity solutions to accelerated flow of real gases for which viscosity is not proportional to temperature and for which Prandtl number is not unity is discussed.

Nomenclature

C = density-viscosity product ratio, $\rho\mu/\rho_e\mu_e$
C_w = surface value, $\rho_w\mu_w/\rho_e\mu_e$
c_f = friction coefficient, $c_f/2 = \tau/\rho_e u_e^2$
f' = dimensionless velocity, u/u_e
f''_w = gradient at surface
G = dimensionless total enthalpy difference; $(g - g_w)/(1 - g_w) = (H_t - H_w)/(H_{t0} - H_w)$
G'_w = gradient at surface, $g'_w/(1 - g_w)$
g = dimensionless total enthalpy, H_t/H_{t0}
g_w = cooling parameter, H_w/H_{t0}
H = static enthalpy
H_t = total enthalpy, $H + u^2/2$
k = thermal conductivity
M = Mach number
Pr = Prandtl number
q = heat flux to surface
r = body or channel radius
Re_s = Reynolds number, $\rho_e u_e s/\mu_e$, where s is $\bar{x}$, θ, or ϕ
S = flow speed parameter, Eq. (5)
St = Stanton number
T = temperature
u,v = components of velocity parallel and normal to surface
x = distance along surface
$\bar{x}$ = length defined in Eq. (10)
y = distance normal to surface
$\bar{\beta}$ = acceleration parameter, Eq. (4)
γ = specific heat ratio
δ = velocity boundary-layer thickness
δ_t = thermal boundary-layer thickness
δ^* = displacement thickness, $\int_0^\infty \left(1 - \frac{\rho u}{\rho_e u_e}\right) dy$
ζ = dimensionless coordinate normal to surface in physical plane, Eq. (9)
η = dimensionless coordinate normal to surface in transformed plane, Eq. (1)
θ = momentum thickness, $\int_0^\infty \frac{\rho u}{\rho_e u_e}\left(1 - \frac{u}{u_e}\right) dy$
μ = viscosity
ξ = coordinate along surface, Eq. (1)
ρ = density
τ = surface shear stress
ϕ = energy thickness, $\int_0^\infty \frac{\rho u}{\rho_e u_e}\left(1 - \frac{H_t - H_w}{H_{t0} - H_w}\right) dy$
ω = exponent of viscosity-temperature relation

Subscripts

aw = adiabatic wall condition
e = condition at freestream edge of boundary layer
o = reservoir condition
t = stagnation condition
w = surface condition

I. Introduction

THE local similarity approach is a relatively simple method for the calculation of heat transfer in accelerated laminar boundary-layer flows over cooled surfaces for a large range of flow speeds. In this method, suggested by Lees,[1] boundary layer profiles at a position along the surface are assumed identical to the similar profiles that would exist for the local freestream condition. This then allows a prediction of heat transfer from the corresponding similarity solution. Subsequently, Back and Witte[2] found this method to be a reasonable approximation for the calculation of heat transfer for a larger range of values of the acceleration parameter $\bar{\beta}$ than Lees considered. Recent calculations by Marvin and Sinclair[3] place the local similarity method on a firmer basis for accelerated flows by their comparison of solutions of the boundary-layer equations with and without the similarity assumption for flow over a cooled, flat-faced body placed in a supersonic main stream. They found little difference between the local similarity method and the solution of the full boundary layer equations in predicting not only the heat transfer but also the wall friction when the boundary layer equations are transformed by the combined Levy-Mangler transformation, as was done by Lees.[1]

These observations spur further interest in similarity solutions for accelerated flows and, by virtue of the local similarity concept, on the nature of boundary-layer velocity and total enthalpy profiles in flows over arbitrary surfaces where, strictly speaking, similarity requirements are not satisfied.

Received May 2, 1969; revision received September 26, 1969. This paper presents the results of one phase of research carried out in the Propulsion Research and Advanced Concepts Section of the Jet Propulsion Laboratory (JPL), California Institute of Technology, under Contract NAS 7-100, sponsored by NASA. The author expresses his gratitude to P. Breckheimer, of JPL, who carried out the numerical calculations.

* Member of the Technical Staff. Associate Fellow AIAA.

Because of surface cooling, acceleration, and lower Reynolds numbers associated with higher altitude flights or higher internal flow temperatures, laminar boundary layers are found over increasingly larger portions of the surface, and even turbulent boundary layers have been found to revert toward laminar boundary layers in regions of flow acceleration under certain conditions, e.g., see Refs. 4–10. Consequently, studies of the effect of acceleration and cooling on the structure of laminar boundary layers seemingly become more important.

In this paper, similarity solutions of the transformed momentum and energy equations are presented for a perfect gas over a large range of freestream velocity variation corresponding to values of $\bar{\beta}$ from 0 to 20, a large range of the cooling parameter g_w from 0 (severely cooled surface) to 1 and encompassing subsonic, transonic and supersonic speeds. Values of $\bar{\beta}$ of 20 are not uncommon in the transonic region in supersonic nozzles[2] and along flat-faced bodies in supersonic flows.[3] Studies of similarity solutions have been restricted to smaller values of $\bar{\beta}$ (Levy,[11] Cohen and Reshotko,[12] Kemp, Rose, and Detra,[13] Beckwith and Cohen,[14] Gross and Dewey,[15] and Dewey and Gross[16] with the largest value of $\bar{\beta}$ of 5 considered by Dewey and Gross. The limiting condition as $\bar{\beta} \to \infty$ has been studied originally by Coles[17] and later by Beckwith and Cohen[14] and Dewey and Gross.[16])

Velocity and total enthalpy profiles are shown in the transformed plane, and the transformation is inverted to display the profiles in the physical plane where they depend upon the flow speed parameter S in addition to $\bar{\beta}$ and g_w. Thicknesses associated with the velocity and thermal layers are presented along with heat-transfer and friction parameters obtained from the profiles. These thicknesses include those of the velocity and total enthalpy layers and those related to boundary-layer displacement and momentum and energy defects. Finally, viscosity and Prandtl number relations for real gases are discussed, since the solutions were obtained for a gas with viscosity proportional to temperature and Prandtl number of unity.

II. Analysis

Application of the combined Levy-Mangler transformation

$$\eta = \frac{r^j \rho_e u_e}{(2\xi)^{1/2}} \int_0^y \frac{\rho}{\rho_e} dy; \quad \xi = \int_0^x \rho_e \mu_e u_e r^{2j} dx \tag{1}$$

to the laminar boundary-layer equations for flow of a perfect gas, e.g., Lees[1] gives the following transformed momentum and energy equations:

$$(Cf'')' + ff'' + \bar{\beta}[g - (f')^2] = 0 \tag{2}$$

$$[(C/Pr)g']' + fg' + S[2C(1 - 1/Pr)f'f'']' = 0 \tag{3}$$

The equations apply to axisymmetric flow with $j = 1$ and to flow over a plane surface with $j = 0$. Implied in these equations is that both the nondimensional velocity $f' = u/u_e$ and total enthalpy $g = H_t/H_{t0}$ depend on the transformed coordinate η, not ξ, and this dependence is the similarity assumption. The primes denote differentiation with respect to η. For variable-property boundary-layer flow over an arbitrary surface, the transformed coordinate η accounts to some extent for property variation across the boundary layer and variable freestream conditions along the surface. These features contribute to the apparent success of the local similarity concept as demonstrated, for example, by Marvin and Sinclair's[3] calculations. For the special case of low-speed, constant-property flow over a flat surface, η is proportional to the distance y normal to the surface divided by the boundary-layer thickness δ and becomes the familiar Blasius similarity variable (e.g., see Schlichting[18]).

For a perfect gas with constant specific heat, the other terms in Eqs. (2) and (3) are as follows:

Density viscosity product

$$C = \rho\mu/\rho_e\mu_e$$

Acceleration parameter

$$\bar{\beta} = \beta(T_{t0}/T_e) = (2\xi/M_e)dM_e/d\xi \text{ where } \beta = (2\xi/u_e)du_e/d\xi \tag{4}$$

Flow speed parameter S, the ratio of kinetic energy to total enthalpy in the freestream,

$$S = \frac{u_e^2}{2H_{t0}} = \frac{\gamma - 1}{2} \frac{M_e^2}{\{1 + [(\gamma - 1)/2]M_e^2\}} \tag{5}$$

To be consistent with the similarity requirements, e.g., Refs. 1, 2, 12, 19, the form of Eqs. (2) and (3) considered herein pertains to a gas with viscosity proportional to temperature ($C = 1$) and Prandtl number of unity, for which Eqs. (2) and (3) become

$$f''' + ff'' + \bar{\beta}[G(1 - g_w) + g_w - (f')^2] = 0 \tag{6}$$

$$G'' + fG' = 0 \tag{7}$$

For convenience, g has been replaced by $G = (g - g_w)/(1 - g_w)$, so that the boundary conditions for flow over an impervious surface at a specified temperature or enthalpy ($g_w = H_w/H_{t0}$) are as follows:

$$\left.\begin{array}{l} \text{At the surface} \\ \qquad \eta = 0\text{: } f(0) = 0, f'(0) = 0, G(0) = 0 \\ \text{Asymptotic condition in freestream as} \\ \qquad \eta \to \infty\text{: } f'(\eta) \to 1, G(\eta) \to 1 \end{array}\right\} \tag{8}$$

The parameters in Eqs. (6) and (7) are $\bar{\beta}$ (acceleration parameter) and g_w (cooling parameter), and the solutions for the velocity and total enthalpy profiles $f'(\eta;\bar{\beta},g_w)$ and $G(\eta;\bar{\beta},g_w)$ are applicable over the entire flow speed range of S from 0 to 1.

Solutions of the coupled nonlinear differential Eqs. (6) and (7), after first being reduced to a system of five first-order equations, were obtained for values of g_w of 0, 0.2, 0.6, 0.8, and 1.0 and values of $\bar{\beta}$ of 0, 0.5, 2, 5, 10, 15, and 20 on a digital computer. The solution method consists of guessing the slopes of the profiles at the surface f''_w and G'_w and integrating the system of equations across the boundary layer to obtain the first approximation that generally does not satisfy the freestream conditions. Subsequent improved iterations were obtained by a method referred to as quasi-linearization, the linearization coming about by expanding the solutions obtained by successive iterations in a Taylor series about the kth iterate and retaining only the first order terms to yield a system that is linear in the $k + 1$ iteration. The application of the method is not described in detail herein but is discussed in Ref. 20 where it was applied to another problem. For larger values of $\bar{\beta}$, the solutions were very difficult to obtain and the reader is referred to Ref. 20 for some discussion in this regard. Other applications of the quasi-linearization to boundary-layer problems have been made by Radbill[21] and Libby and Chen[22] for isothermal flow, and by Libby,[23] Libby and Liu,[24] and Back,[25] including heat transfer. Confidence in the solution method is established for small values of $\bar{\beta}$ by coincidence of the profile slopes at the surface f''_w and G'_w with values that have been previously obtained.[12,14,16]

III. Results

A. Profiles

To indicate the nature of the solutions in the transformed coordinate η, velocity and total enthalpy profiles are shown

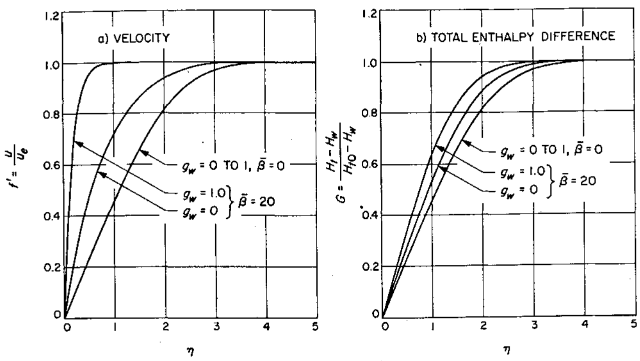

Fig. 1 Velocity and total enthalpy profiles in the transformed plane.

in Fig. 1. For a constant freestream velocity $\bar{\beta} = 0$, the profiles are invariable with cooling, i.e., with g_w. The profiles become steeper near the surface with acceleration and, at a particular value of the acceleration parameter $\bar{\beta}$, they become less steep with cooling. Both acceleration and cooling influence the velocity profiles more than the total enthalpy profiles.

The actual effect of cooling on the profiles in the physical plane is opposite to that seen in Fig. 1 in the transformed plane. When the transformation Eq. (1) is inverted, the coordinate ζ, related to the physical x, y plane, is given by

$$\zeta = \frac{y}{\bar{x}} (Re_{\bar{x}})^{1/2} = 2^{1/2} \int_0^{\eta} \frac{\rho_e}{\rho} d\eta \tag{9}$$

The length $\bar{x}$ was introduced to cast the results in a form familiar for low-speed constant-property laminar boundary layers, $\bar{x}$ being defined by

$$\bar{x} = \xi / \rho_e \mu_e u_e r^{2j} = \int_0^x \rho_e \mu_e u_e r^{2j} dx \Big/ \rho_e \mu_e u_e r^{2j} \tag{10}$$

and $Re_{\bar{x}}$ is the Reynolds number based on local freestream conditions, $\rho_e u_e \bar{x} / \mu_e$. The velocity and total enthalpy profiles in the coordinate ζ also depend upon the flow speed parameter S, i.e., $f'(\zeta;\bar{\beta},g_w,S)$ and $G(\zeta;\bar{\beta},g_w,S)$ since the

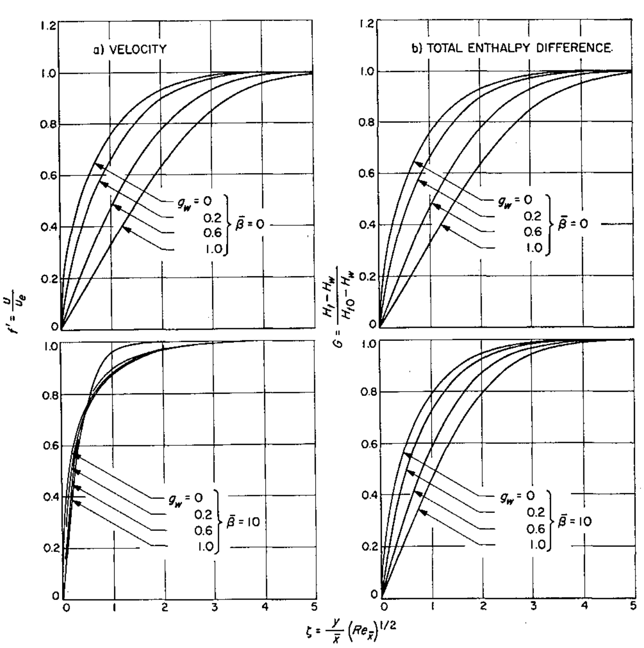

Fig. 2 Effect of cooling on the velocity and total enthalpy profiles in the physical plane; constant freestream velocity ($\bar{\beta} = 0$) and with acceleration ($\bar{\beta} = 10$); low-speed limit $S \rightarrow 0$.

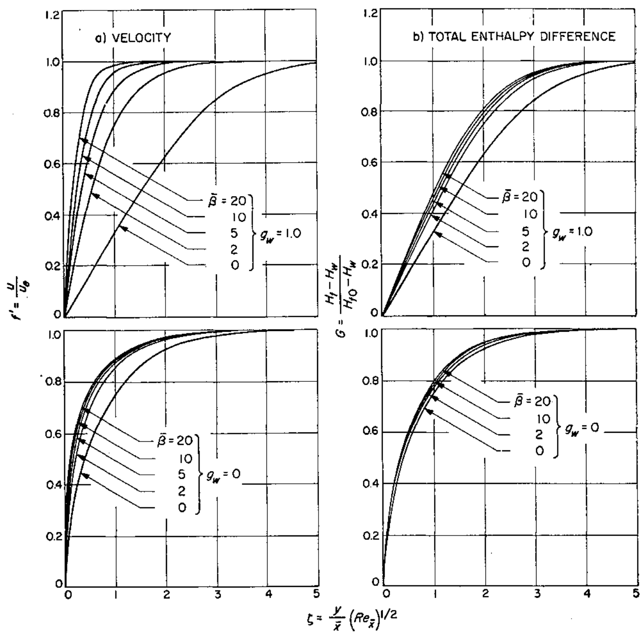

Fig. 3 Effect of acceleration on the velocity and total enthalpy profiles in the physical plane; constant properties ($g_w = 1.0$) and severely cooled surface ($g_w = 0$); low-speed limit $S \rightarrow 0$.

density ratio is given by

$$\frac{\rho_e}{\rho} = \frac{G(1 - g_w) + g_w - S(f')^2}{1 - S} \tag{11}$$

Values of $S \rightarrow 0$, 0.25, 0.50, 0.75, and 0.90 were investigated over the range of $\bar{\beta}$ from 0 to 20 and g_w from 0 to 1. Only a sample of the numerous boundary-layer profiles that were obtained (140 conditions involving various values of $\bar{\beta}, g_w$, and S) is shown.

The effect of cooling on the profiles in the physical plane is shown in Fig. 2. The profiles become steeper near the surface with cooling and have more curvature. This trend

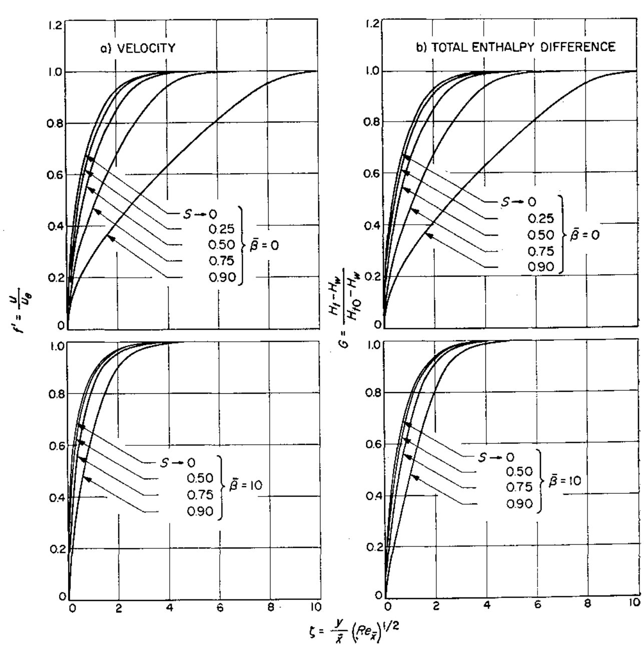

Fig. 4 Effect of flow speed on the velocity and total enthalpy profiles in the physical plane; constant freestream velocity ($\bar{\beta} = 0$), and with acceleration ($\bar{\beta} = 10$); severely cooled surface ($g_w = 0$).

Table 1 Acceleration and cooling results, independent of flow speed S

$\bar{\beta}$	g_w	G'_w	f''_w	$\frac{\theta}{\bar{x}}(Re_{\bar{x}})^{1/2}$	$\frac{\phi}{\theta}$	$St\,Re_\phi$	$\frac{c_f}{2}Re_\theta$	$St/\left(\frac{c_f}{2}\right)$
0	0	0.46960	0.46960	0.664	1.000	0.221	0.221	1.0
↓	0.2	↓	↓	↓	↓	↓	↓	↓
	0.6							
	0.8							
	1.0							
0.5	0	0.49424	0.58116	0.599	1.166	0.244	0.246	0.850
↓	0.2	0.50451	0.65497	0.579	1.232	0.254	0.268	0.770
	0.6	0.52285	0.79520	0.538	1.375	0.273	0.302	0.658
	0.8	0.53092	0.86226	0.516	1.458	0.283	0.315	0.616
	1.0	0.53899	0.92768	0.495	1.539	0.290	0.325	0.581
2	0	0.52064	0.73865	0.542	1.357	0.271	0.283	0.705
↓	0.2	0.54173	0.94833	0.502	1.524	0.293	0.337	0.571
	0.6	0.57657	1.3334	0.416	1.958	0.332	0.393	0.432
	0.8	0.59089	1.5134	0.372	2.266	0.352	0.398	0.390
	1.0	0.60520	1.6872	0.326	2.622	0.366	0.389	0.359
5	0	0.53886	0.89068	0.516	1.477	0.290	0.325	0.605
↓	0.2	0.56824	1.2816	0.464	1.732	0.323	0.420	0.443
	0.6	0.61438	1.9824	0.348	2.500	0.377	0.487	0.310
	0.8	0.63353	2.3056	0.286	3.134	0.401	0.466	0.275
	1.0	0.65088	2.6158	0.224	4.116	0.424	0.414	0.249
10	0	0.55100	1.0308	0.504	1.545	0.304	0.368	0.535
↓	0.2	0.58664	1.6422	0.446	1.862	0.344	0.517	0.357
	0.6	0.64057	2.7162	0.309	2.928	0.410	0.594	0.236
	0.8	0.66248	3.2066	0.237	3.959	0.439	0.536	0.207
	1.0	0.68217	3.6752	0.163	5.921	0.465	0.423	0.186
15	0	0.55717	1.1231	0.500	1.575	0.310	0.397	0.496
↓	0.2	0.59632	1.9114	0.439	1.923	0.356	0.593	0.312
	0.6	0.65432	3.2789	0.292	3.165	0.428	0.678	0.200
	0.8	0.67763	3.8996	0.214	4.475	0.459	0.591	0.174
	1.0	0.69848	4.4915	0.134	7.349	0.488	0.427	0.156
20	0	0.56110	1.1935	0.499	1.592	0.315	0.421	0.470
↓	0.2	0.60265	2.1348	0.435	1.959	0.363	0.657	0.282
	0.6	0.66328	3.7528	0.282	3.324	0.440	0.749	0.177
	0.8	0.68747	4.4843	0.200	4.850	0.473	0.636	0.153
	1.0	0.70907	5.1807	0.117	8.570	0.503	0.429	0.137
∞ [a]	0	0.5901	∞	0.504 [b]		0.3482	∞ [b]	0
↓	0.2	0.6590	↓			0.4343	↓	↓
	0.6	0.7408				0.5488		
	1.0	0.7979		0		0.6366	0.435	

[a] Coles'[17] values corrected as in Back and Witte.[2]
[b] Dewey and Gross.[16]

is also found with acceleration ($\bar{\beta} = 10$), but the effect is less on the velocity than the total enthalpy profiles. Since the velocity boundary-layer thickness increases with cooling at larger values of $\bar{\beta}$, the velocity profiles cross over in the outer part of the boundary layer.

The effect of acceleration on the velocity and total enthalpy profiles in the physical plane is shown in Fig. 3. Similar to the profiles shown in the transformed plane, the profiles become steeper near the surface with acceleration. The spread of the profiles with $\bar{\beta}$ decreases with cooling, and the total enthalpy profiles are virtually unaffected by acceleration for a severely cooled surface ($g_w = 0$).

The profiles shown in Figs. 2 and 3 were for negligibly small values of the flow speed parameter S. The effect of flow speed on the profiles in the physical plane is shown in Fig. 4 for a severely cooled surface ($g_w = 0$). For a constant freestream velocity ($\bar{\beta} = 0$), there is considerable thickening of the boundary layer owing to viscous dissipation, and both profiles become flatter in the outer portion of the boundary layer. Profiles are not shown for less surface cooling, but the dissipative effect is more pronounced. With acceleration ($\bar{\beta} = 10$) the effect of flow speed is not large, there being hardly any difference in the profiles for $S \rightarrow 0$ to 0.50.

B. Thicknesses

Velocity and thermal layer thicknesses, δ and δ_t, were obtained by using Eqs. (9) and (11), and displacement, momentum, and energy thicknesses, δ^*, θ, and ϕ, in the physical x, y plane were obtained by using Eq. 1 as follows:

$$\frac{\delta}{\bar{x}}(Re_{\bar{x}})^{1/2} = 2^{1/2}\int_0^{\eta_{f'=0.99}}\left[\frac{G(1-g_w)+g_w-S(f')^2}{1-S}\right]d\eta \tag{12}$$

$$\frac{\delta_t}{\bar{x}}(Re_{\bar{x}})^{1/2} = 2^{1/2}\int_0^{\eta_{G=0.99}}\left[\frac{G(1-g_w)+g_w-S(f')^2}{1-S}\right]d\eta \tag{13}$$

$$\frac{\delta^*}{\bar{x}}(Re_{\bar{x}})^{1/2} = 2^{1/2}\int_0^{\infty}\left[\frac{G(1-g_w)+g_w-S(f')^2}{1-S} - f'\right]d\eta \tag{14}$$

$$\frac{\theta}{\bar{x}}(Re_{\bar{x}})^{1/2} = 2^{1/2}\int_0^{\infty} f'(1-f')d\eta \tag{15}$$

$$\frac{\phi}{\bar{x}}(Re_{\bar{x}})^{1/2} = 2^{1/2}\int_0^{\infty} f'(1-G)d\eta \tag{16}$$

The integrals appearing in these relations were evaluated using Simpson's formula. The momentum and energy thickness groups depend on the acceleration and cooling parameters $\bar{\beta}$ and g_w, while the velocity and thermal boundary-layer thicknesses and displacement thickness groups depend, in addition, on the flow speed parameter S. Tables 1 and 2 contain results of the thickness calculations, and some of the values are shown in Figs. 5–8 to display the trends that are not as easily discernible in the Tables.

Table 2 Acceleration, cooling, and flow speed results

$\bar{\beta}$	g_w	$\frac{\delta^*}{\bar{x}}(Re_{\bar{x}})^{1/2}$ S = 0	0.25	0.50	0.75	0.90	$\frac{\delta}{\bar{x}}(Re_{\bar{x}})^{1/2}$ S = 0	0.25	0.50	0.75	0.90	δ_t/δ S = 0	0.25	0.50	0.75	0.90
0	0	0	0.221	0.664	1.992	5.977	3.193	3.413	3.853	5.171	9.127	1.0	1.0	1.0	1.0	1.0
	0.2	0.344	0.680	1.352	3.368	9.415	3.533	3.867	4.535	6.540	12.55					
	0.6	1.032	1.598	2.728	6.120	16.30	4.219	4.782	5.908	9.285	19.42					
	0.8	1.376	2.056	3.416	7.495	19.73	4.562	5.240	6.594	10.66	22.85					
	1.0	1.720	2.515	4.104	8.873	23.18	4.906	5.697	7.280	12.03	26.28					
0.5	0	-0.154	-0.0060	0.291	1.181	3.850	2.895	3.042	3.337	4.222	6.877	1.070	1.066	1.061	1.048	1.030
	0.2	0.115	0.347	0.809	2.198	6.364	3.121	3.351	3.812	5.194	9.340	1.085	1.079	1.070	1.052	1.030
	0.6	0.636	1.028	1.810	4.158	11.20	3.533	3.923	4.702	7.038	14.05	1.116	1.104	1.088	1.059	1.031
	0.8	0.889	1.357	2.294	5.106	13.54	3.719	4.185	5.118	7.915	16.31	1.138	1.123	1.101	1.067	1.034
	1.0	1.138	1.682	2.771	6.037	15.84	3.888	4.429	5.511	8.758	18.50	1.151	1.133	1.108	1.069	1.035
2	0	-0.292	-0.208	-0.0408	0.461	1.966	2.675	2.758	2.925	3.426	4.929	1.126	1.122	1.115	1.098	1.069
	0.2	-0.0832	0.0566	0.336	1.175	3.691	2.805	2.945	3.224	4.061	6.573	1.160	1.153	1.140	1.111	1.069
	0.6	0.318	0.563	1.053	2.522	6.929	2.943	3.187	3.676	5.142	9.540	1.264	1.244	1.211	1.152	1.083
	0.8	0.511	0.806	1.394	3.160	8.457	2.910	3.204	3.791	5.553	10.84	1.372	1.339	1.287	1.197	1.103
	1.0	0.703	1.047	1.733	3.793	9.972	2.753	3.094	3.774	5.816	11.94	1.510	1.455	1.375	1.246	1.124
5	0	-0.367	-0.317	-0.218	0.0793	0.972	2.599	2.649	2.748	3.045	3.937	1.140	1.138	1.133	1.120	1.093
	0.2	-0.194	-0.104	0.0755	0.615	2.233	2.694	2.783	2.963	3.502	5.120	1.181	1.175	1.165	1.139	1.095
	0.6	0.144	0.307	0.635	1.617	4.564	2.713	2.876	3.204	4.185	7.131	1.326	1.307	1.276	1.211	1.124
	0.8	0.309	0.507	0.904	2.093	5.663	2.510	2.709	3.105	4.293	7.859	1.512	1.474	1.414	1.300	1.164
	1.0	0.471	0.703	1.167	2.557	6.727	1.953	2.182	2.641	4.017	8.145	2.042	1.934	1.773	1.512	1.258
10	0	-0.409	-0.377	-0.314	-0.123	0.449	2.568	2.600	2.663	2.854	3.426	1.143	1.142	1.138	1.129	1.108
	0.2	-0.258	-0.195	-0.0703	0.305	1.431	2.647	2.710	2.835	3.210	4.336	1.186	1.181	1.173	1.153	1.113
	0.6	0.0438	0.161	0.397	1.103	3.222	2.630	2.747	2.983	3.689	5.808	1.340	1.326	1.300	1.243	1.154
	0.8	0.193	0.336	0.623	1.482	4.061	2.370	2.513	2.799	3.659	6.237	1.566	1.534	1.479	1.367	1.215
	1.0	0.341	0.508	0.844	1.851	4.872	1.440	1.606	1.938	2.934	5.921	2.702	2.527	2.268	1.841	1.423
15	0	-0.428	-0.404	-0.355	-0.210	0.225	2.555	2.579	2.627	2.772	3.207	1.145	1.143	1.141	1.133	1.115
	0.2	-0.288	-0.237	-0.137	0.165	1.071	2.627	2.677	2.778	3.079	3.985	1.187	1.184	1.177	1.160	1.124
	0.6	-0.0027	0.0938	0.287	0.866	2.604	2.598	2.695	2.888	3.467	5.205	1.343	1.331	1.309	1.257	1.171
	0.8	0.139	0.257	0.493	1.199	3.319	2.328	2.445	2.681	3.388	5.508	1.577	1.549	1.501	1.397	1.244
	1.0	0.280	0.418	0.695	1.523	4.010	1.191	1.328	1.601	2.420	4.879	3.230	3.002	2.662	2.103	1.553
20	0	-0.439	-0.419	-0.380	-0.261	0.0961	2.547	2.567	2.607	2.726	3.082	1.145	1.144	1.142	1.136	1.120
	0.2	-0.306	-0.263	-0.177	0.0818	0.857	2.615	2.658	2.744	3.002	3.777	1.188	1.185	1.179	1.164	1.130
	0.6	-0.0310	0.0527	0.220	0.723	2.230	2.579	2.663	2.830	3.333	4.840	1.346	1.335	1.315	1.267	1.184
	0.8	0.107	0.209	0.414	1.028	2.870	2.306	2.408	2.613	3.227	5.070	1.582	1.557	1.513	1.416	1.265
	1.0	0.243	0.364	0.604	1.325	3.487	1.036	1.155	1.392	2.105	4.242	3.689	3.414	3.004	2.330	1.666

The large effect of acceleration, flow speed, and cooling on the displacement thickness group $(\delta^*/\bar{x})(Re_{\bar{x}})^{1/2}$ is shown in Fig. 5. Acceleration considerably reduces the displacement thickness group, whereas the effect of flow speed is to increase the group. For a severely cooled surface ($g_w = 0$) these same trends are found, but the dependence on acceleration and flow speed is less. Over a large range of values of $\bar{\beta}$ and S, the displacement thickness is negative with severe cooling, because the mass flux through the boundary layer exceeds the local freestream value.

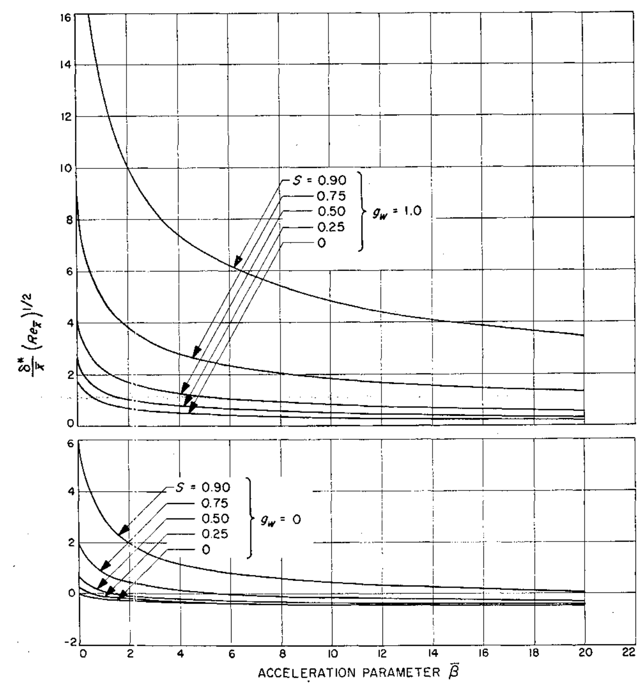

Fig. 5 Effect of acceleration and flow speed on displacement thickness (g_w = 1.0) and severely cooled surface (g_w = 0).

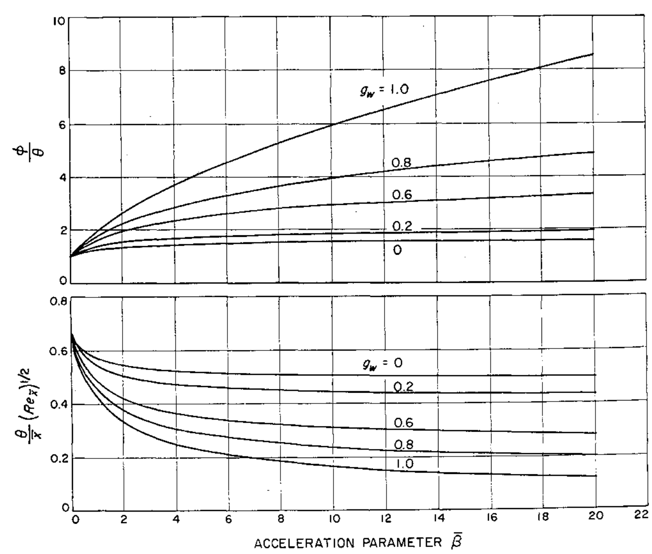

Fig. 6 Effect of acceleration and cooling on the momentum and energy thickness relations, independent of flow speed S.

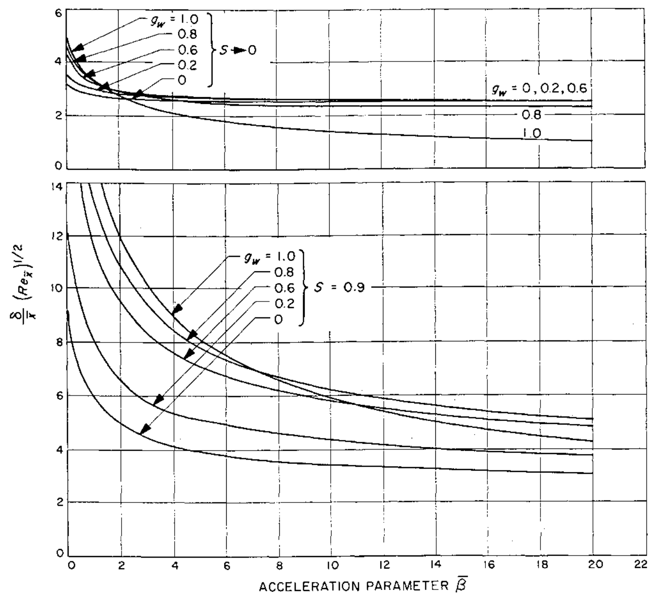

Fig. 7 Effect of acceleration and cooling on velocity boundary-layer thickness; low-speed limit $S \to 0$, and high-speed case $S = 0.9$.

The momentum thickness group $(\theta/\bar{x})(Re_{\bar{x}})^{1/2}$ (Fig. 6) decreases with acceleration and, at a particular value of $\bar{\beta}$, increases with cooling, unlike the displacement thickness group (Fig. 5 and Table 2). This behavior occurs because the mass flux through the boundary layer increases with cooling, and consequently the mass flux defect is less, but the momentum defect is greater. With acceleration the energy thickness exceeds the momentum thickness (Fig. 6), the ratio ϕ/θ being as large as 8.6 at $\bar{\beta} = 20$ and $g_w = 1.0$. Cooling reduces the ratio between ϕ and θ, and for severe cooling the ratio ϕ/θ is nearly invariable with acceleration.

For relatively small values of the acceleration parameter $\bar{\beta}$, the influence of cooling on the velocity boundary layer thickness group $(\delta/\bar{x})(Re_{\bar{x}})^{1/2}$ (Fig. 7) is similar to that on the displacement group. However, at larger values of $\bar{\beta}$, the trend with cooling changes: the group $(\delta/\bar{x})(Re_{\bar{x}})^{1/2}$ first increases with cooling, reaches a maximum, and then decreases slightly with cooling. This behavior is dependent on the flow speed parameter S (Fig. 7 and Table 2). Similar to the ratio ϕ/θ, the thermal boundary layer thickness δ_t exceeds the velocity boundary layer thickness δ with acceleration (Fig. 8). Note that this trend is independent of any Prandtl number effect since Pr = 1. Instead, for a particular value of g_w and S, the group $(\delta/\bar{x})(Re_{\bar{x}})^{1/2}$ decreases significantly with acceleration while the group $(\delta_t/\bar{x})(Re_{\bar{x}})^{1/2}$ decreases less; consequently, the ratio δ_t/δ increases. The ratio δ_t/δ also depends on the flow speed parameter S, the effect of flow speed being to equalize the thicknesses δ_t and δ. Other quantities of interest, such as δ^*/θ (shape factor), θ/δ, ϕ/δ_t, etc., can be obtained from the values in Tables 1 and 2.

C. Friction and Heat Transfer

The surface shear stress and heat flux to the surface are, respectively,

$$\tau = \mu_w \left(\frac{\partial u}{\partial y}\right)_w = \mu_w u_e \left(\frac{\partial \eta}{\partial y}\right)_w \left(\frac{df'}{d\eta}\right)_w =$$

$$\rho_e u_e^2 \left[\frac{r^j \mu_e}{(2\xi)^{1/2}}\right] C_w f''_w \quad (17)$$

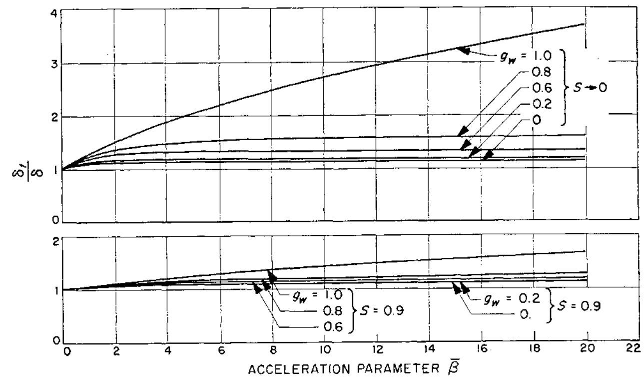

Fig. 8 Effect of acceleration and cooling on the ratio of thermal to velocity boundary-layer thickness δ_t/δ; low-speed limit $S \to 0$, and high-speed case $S = 0.9$.

and

$$q = k_w \left(\frac{\partial T}{\partial y}\right)_w = \frac{\mu_w}{Pr} H_{t0} \left(\frac{\partial \eta}{\partial y}\right)_w \left(\frac{dg}{d\eta}\right)_w =$$

$$(H_{t0} - H_w)(\rho_e u_e) \left[\frac{r^j \mu_e}{(2\xi)^{1/2}}\right] \frac{C_w}{Pr} \left(\frac{g'_w}{1 - g_w}\right) \quad (18)$$

Consistent with the assumptions that viscosity is proportional to temperature ($C = C_w = 1$) and that $Pr = 1$, the shear stress and heat flux can be written in terms of the friction coefficient and Stanton number:

$$c_f/2 = \tau/\rho_e u_e^2 = [1/(Re_{\bar{x}})^{1/2}] f''_w/2^{1/2} \quad (19)$$

and

$$St = q/(H_{t0} - H_w)(\rho_e u_e) = [1/(Re_{\bar{x}})^{1/2}] G'_w/2^{1/2} \quad (20)$$

The quantities f''_w and $G'_w = g'_w/(1 - g_w)$ are the slopes of the normalized velocity and total enthalpy difference profiles at the surface in the transformed plane, and are shown in Figs. 9 and 10, respectively. Both of these quantities increase with acceleration and decrease with cooling, although both acceleration and cooling influence the friction parameter f''_w more than the heat transfer parameter G'_w. In fact, for a severely cooled surface ($g_w = 0$), the heat transfer parameter G'_w increases by only about 25% from $\bar{\beta} =$ 0 to ∞. This weak dependence formed the basis for suggesting an approximate method of predicting heat transfer to highly cooled surfaces by applying the similarity solutions on a local basis to accelerated flows with higher values of $\bar{\beta}$ (Back and Witte[2]) as had been previously proposed by Lees[1] for accelerated flows with $\bar{\beta}$ up to 2. The small variation of the heat-transfer parameter G'_w with g_w also indicates that

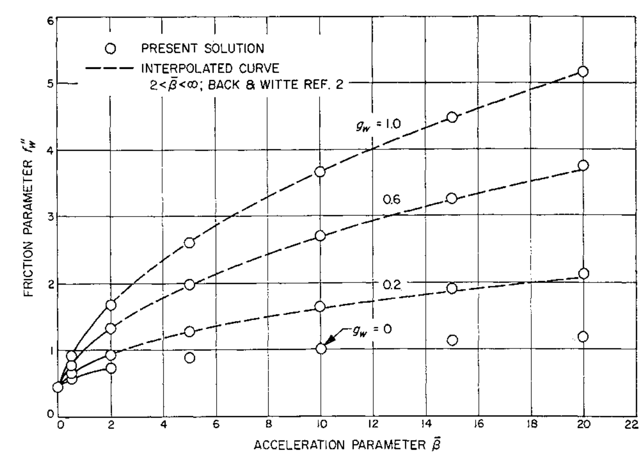

Fig. 9 Variation of the friction parameter f_w'' with acceleration and cooling, independent of flow speed S.

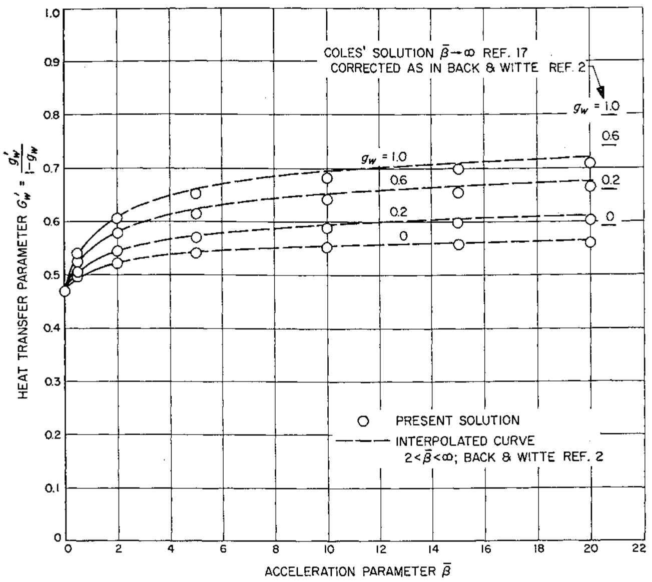

Fig. 10 Variation of the heat-transfer parameter G_w' with acceleration and cooling, independent of flow speed S.

the heat transfer might be predicted for surfaces that are not necessarily isothermal, as long as g_w is small.

The present solutions allow an appraisal of the interpolated values for f''_w and G'_w that were obtained by Back and Witte[2] using Cohen and Reshotko's[12] solutions for $\bar{\beta}$ up to 2 and Coles'[17] limiting solutions as $\bar{\beta} \to \infty$. The agreement is excellent for the friction parameter f''_w as seen in Fig. 9 (interpolated values were not possible for $g_w = 0$), but are slightly inferior for the heat transfer parameter G'_w (Fig. 10) where differences of 2% at most are found for g_w near 1. Consequently, the present calculations add credence to those interpolated values of f''_w and G'_w that were given by Back and Witte[2] for calculation purposes. More accurate values can be obtained from Table 1.

The ratio of the Stanton number to the friction coefficient, referred to as the Reynolds analogy factor, is given by

$$St/(c_f/2) = G'_w/f''_w \tag{21}$$

and is shown in Fig. 11. This factor is considerably reduced by acceleration, but the decrease is less with cooling.

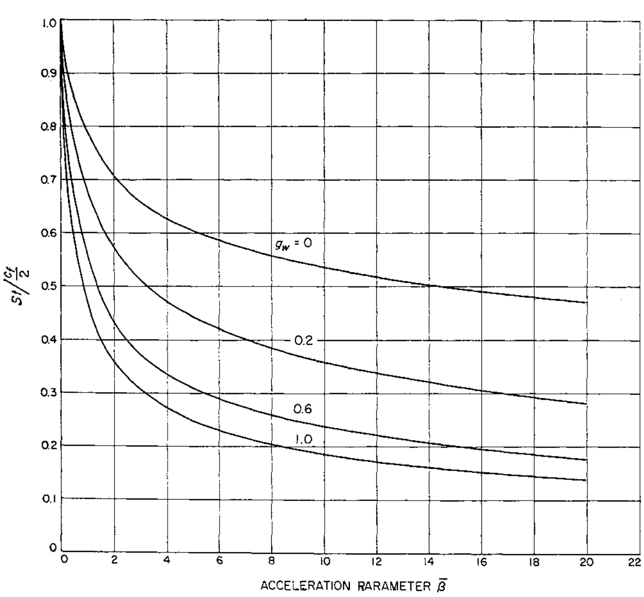

Fig. 11 Effect of acceleration and cooling on the Reynolds analogy factor; independent of flow speed S.

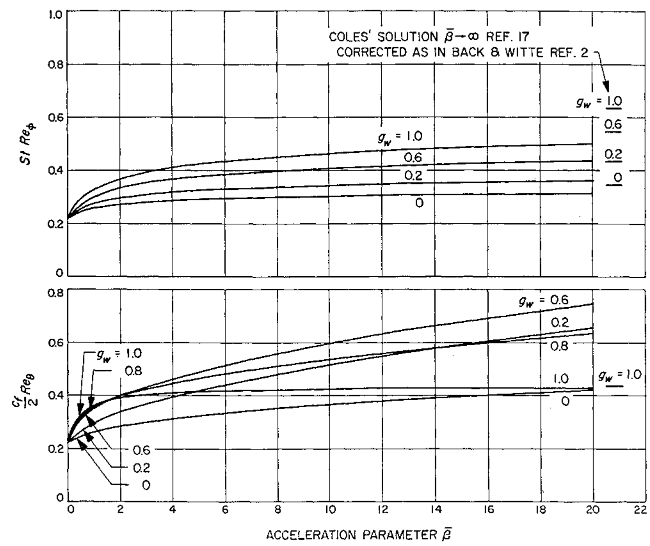

Fig. 12 Heat-transfer and friction groups with acceleration and cooling; independent of flow speed S.

A final view of the calculations is shown in Fig. 12 in terms of the friction coefficient/momentum thickness Reynolds number group and the Stanton number/energy thickness Reynolds number group. These groups are given by combining Eqs. (15) and (19) and Eqs. (16) and (20) as follows:

$$\frac{c_f}{2}Re_\theta = f''_w\int_0^\infty f'(1 - f')d\eta \tag{22}$$

$$St\,Re_\phi = G'_w\int_0^\infty f'(1 - G)d\eta = (G'_w)^2 \tag{23}$$

The double equality in Eq. (23) follows from integration of the energy Eq. (7) across the boundary layer. Both of these groups, which are useful in obtaining or appraising solutions of the integral form of the momentum and energy equations by approximate methods, increase with acceleration, but while the heat transfer group $St\,Re_\phi$ decreases with cooling, similar to $St(Re_{\bar{x}})^{1/2} = G'_w/2^{1/2}$, a more complicated dependence on cooling is indicated for the friction group $(c_f/2)Re_\theta$ at small and large values of the acceleration parameter $\bar{\beta}$.

IV. Viscosity and Prandtl Number Considerations

It was possible to obtain similarity solutions over a range of flow speeds by taking the viscosity proportional to temperature and the Prandtl number equal to unity. However, for most real gases, these ideal situations are generally not true and one inquires to what extent the results presented herein are applicable to real gases for which the viscosity dependence on temperature is usually less than linear and the Prandtl number is usually less than unity. This question is difficult to answer because there are virtually no investigations of the effect of viscosity and Prandtl number for the kind of flow acceleration considered herein. Investigations of the influence of various viscosity-temperature relations (such as the Sutherland law and the empirical relation $\mu \propto T^\omega$) and of Prandtl numbers less than unity have been made, but only for flat-plate flow for small values of the acceleration parameter. A survey of these investigations is beyond the scope of this paper; however, some comments seem appropriate with regard to effects that have been found.

The viscosity enters in the similarity equations in terms of the density-viscosity product $C = (\rho\mu)/(\rho_e\mu_e)$ that appears as a coefficient of both f'' and g' in the momentum and energy Eqs. (2) and (3) and also in the flow speed term in the

Table 3 Effect of viscosity-temperature relation on previous wall friction and heat-transfer predictions

Source	Flow regime	Freestream velocity condition	Finding
Back[25] Cooling and heating, $g_w = 0.01$–10, $Pr = \frac{2}{3}$, $\omega = 0.75$ and 1	Low speed limit, $S \to 0$	Constant freestream velocity, $\bar{\beta} = 0$	Small effect, e.g., at $g_w = 0.01$, $St(Re_x)^{1/2}$ and $(c_f/2)(Re_x)^{1/2}$ for $\omega = 0.75$ exceeded values for $\omega = 1.0$ by about 10%
Hantzche and Wendt[18] Adiabatic wall, $Pr = 1$, $\omega = 0.5$–1 Crocco[26] g_w down to 0.25, $Pr = 0.725$ $\omega = 0.5$–1.25 and Sutherland law	Compressible	$\bar{\beta} = 0$	$(c_f/2)(Re_x)^{1/2}$ independent of M and Pr for $\omega = 1.0$. For $\omega < 1$, $(c_f/2)(Re_x)^{1/2}$ decreases with M and increases with cooling, but effect not large, e.g., at $M = 5$ and $Pr = 0.725$, $(c_f/2)(Re_x)^{1/2}$, for $\omega = 0.75$, is lower by 16 and 4%, respectively, for an adiabatic and cooled wall ($g_w = 0.25$) than for $\omega = 1.0$. Similar remarks apply to $St(Re_x)^{1/2}$ for $Pr = 1$; for $Pr < 1$, Colburn analogy $St\ Pr^{2/3} = c_f/2$ applies (Eckert[27])
Fay and Riddell[28] Air, g_w down to 0.01 $Pr = 0.71$ Back and Witte,[2] in conjunction with Bade's[29] calculations, $g_w = 0.01$–0.8, $Pr = \frac{2}{3}$ $\omega = 0.5$ to 1.0	$S \to 0$	Stagnation point $\bar{\beta} = \frac{1}{2}$	Weak dependence indicated by small correction factor $(\rho_w\mu_w/\rho_e\mu_e)^{0.1}$ to heat-transfer prediction
Gross and Dewey[15] g_w down to 0.15, $Pr = 0.5$–1 $\omega = 0.5$–1 and Sutherland law	$S \to 0$ and 1	$\bar{\beta} = 0$ and 1	In hypersonic limit $S \to 1$ hardly any difference in predicted friction and heat transfer with appreciable cooling ($g_w = 0.15$) for small value of $\bar{\beta} = 1$, but 20% difference for constant freestream velocity $\bar{\beta} = 0$
Dewey and Gross[16] g_w down to 0, $Pr = 0.5$–1 $\omega = 0.5$–1 and Sutherland law	$S \to 0$–1	$\bar{\beta}$ to 3 for $\omega < 1$	Predicted friction and heat transfer hardly affected in low speed limit ($S \to 0$) as acceleration parameter $\bar{\beta}$ was increased

energy equation. For the empirical relation $\mu \propto T^{\omega}$, C can be written in the form

$$C = \{(1 - S)/[G(1 - g_w) + g_w - S(f')^2]\}^{1-\omega}$$

The similarity requirement is satisfied only if $\omega = 1$, i.e., $\mu \propto T$ for which $C = 1$. Clearly, the similarity solutions become less accurate when applied to a real gas if ω becomes less than 1 and, for a given value of ω, both cooling g_w and flow speed S influence the results.

An indication of the influence of the viscosity-temperature relation on the predicted wall friction and heat transfer from previous investigations is given in Table 3. Examination of the results indicates the effect to be relatively small, especially with flow acceleration. Clearly, for real gas flows subjected to the kind of flow acceleration considered herein, the effect of flow acceleration is generally larger than any inference that might be made about the effect of viscosity law.

Although the effect of Prandtl number, like that of the viscosity law, has not been investigated for the kind of flow acceleration considered herein, the dependence of heat transfer on Prandtl number is known to be significant enough for a correction to be made by including the factor $Pr^{2/3}$ in those expressions that involve the Stanton number; i.e., St should be replaced by $St\ Pr^{2/3}$. The Stanton number appears in Eqs. (20, 21, and 23), in Table 1, and in Figs. 11 and 12. This factor is indicated by the constant-property, low-speed flat-plate flow solution of Pohlhausen (e.g., see Schlichting[18]) and for variable-property flat-plate flow provided that $\mu \propto T$ by virtue of the transformation of the laminar boundary layer equations to constant-property form (Eqs. (2) and (3) with $\bar{\beta} = 0$, $C = 1$, $S \to 0$). The calculations by Gross and Dewey,[15] who also investigated a range of Prandtl numbers from 0.5 to 1, support the trend indicated by this factor, although the exponent in the factor varies somewhat. Other exponents have been recommended; e.g., Fay and Riddell[28] give $Pr^{0.6}$ a factor differing slightly from $Pr^{2/3}$.

To be consistent with the Prandtl number correction, the enthalpy difference $(H_{t0} - H_w)$ in the Stanton number [Eq. (20)] should be replaced by the difference between adiabatic wall and wall enthalpies $(H_{aw} - H_w)$. The adiabatic wall enthalpy can be calculated as usual from a recovery factor $R = (H_{aw} - H_e)/(H_{t0} - H_e) = Pr^{1/2}$. Kemp, Rose and Detra[13] found this recovery factor dependence on Prandtl number (their calculations were made for $Pr = 0.71$) to be valid over a large flow speed range of S to 0.75 for air with $\rho\mu$ variable and for a value of the acceleration parameter $\bar{\beta}$ up to 2. The calculations by Kemp, Rose and Detra,[13] who chose to vary the acceleration and flow speed parameters at will with $\rho\mu$ variable and Prandtl number not equal to unity in Eqs. (2) and (3), also indicated, in particular for cooled surfaces (g_w from 0.01 to 0.17), that the heat transfer parameter G'_w was only slightly affected by values of S ranging up to 0.75 and was mainly affected by $\bar{\beta}$ for the range of $\bar{\beta}$ to 2 investigated.

Other quantities associated with the thermal boundary layer, such as the energy thickness ϕ and thermal boundary layer thickness δ_t, would exceed those values shown in Tables 1 and 2 and Figs. 6 and 8 for a Prandtl number less than unity. For example, the calculations by Back[25] for a $Pr = \frac{2}{3}$ indicate the ratio ϕ/θ to be about 1.3 over a range of cooling from $g_w = 0.01$ to 1 for low-speed flow with constant freestream velocity. Over the same range of cooling, δ_t/δ increased slightly with cooling, being at most 10% above the constant-property relation $\delta_t/\delta = Pr^{-1/3} = 1.15$ for $Pr = \frac{2}{3}$.

V. Summary and Conclusions

Similarity solutions of the laminar boundary layer equations were obtained for flow of a perfect gas over an isothermal surface for a large range of flow acceleration, surface cooling, and flow speeds. The Levy-Mangler transformation was applied to the boundary-layer equations, the equations were solved numerically in the transformed plane, and then the solutions were inverted and shown in the physical plane.

The velocity and total enthalpy profiles change markedly with the parameters $\bar{\beta}$ (acceleration), g_w (cooling), and S (flow speed or compressibility). The effect of acceleration and cooling is to steepen the profiles near the surface and to increase their curvature, while the effect of flow speed is opposite to this. In general, effects found with acceleration were less with simultaneous cooling, and both acceleration and cooling reduced flow speed or compressibility effects. Thicknesses associated with the boundary layer were found to be strongly dependent on the acceleration, cooling, and flow speed parameters. The friction and heat-transfer parameters, which increased with acceleration and decreased with cooling, were in good agreement with interpolated values previously available for $\bar{\beta}$ greater than 2.

To apply the similarity solutions to an accelerated flow of a real gas with viscosity not proportional to temperature and Prandtl number not equal to unity, a correction for the heat transfer dependence on Prandtl number is suggested. Utilization of the similarity solutions on a local basis to predict the quantities of interest, in particular the heat transfer that is weakly dependent on the acceleration parameter $\bar{\beta}$ and cooling parameter g_w as long as g_w is small, requires the evaluation of length $\bar{x}$ from Eq. (10) and parameters $\bar{\beta}$ and g_w, once the freestream variables are specified along the surface.

References

[1] Lees, L., "Laminar Heat Transfer Over Blunt-Nosed Bodies at Hypersonic Flight Speeds," *Jet Propulsion*, Vol. 26, 1956, pp. 259–269.

[2] Back, L. H. and Witte, A. B., "Prediction of Heat Transfer From Laminar Boundary Layers, With Emphasis on Large Free-Stream Velocity Gradients and Highly Cooled Walls," *Transactions of the ASME, Ser. C: Journal of Heat Transfer*, Vol. 88, Aug. 1966, pp. 249–256.

[3] Marvin, J. G. and Sinclair, A. R., "Convective Heating in Regions of Large Favorable Pressure Gradient," *AIAA Journal*, Vol. 5, No. 11, Nov. 1967, pp. 1940–1948.

[4] Launder, B. E., "Laminarization of the Turbulent Boundary Layer by Acceleration," Rept. 77, 1964, Massachusetts Institute of Technology, Gas Turbine Lab., Cambridge, Mass.

[5] Moretti, P. M. and Kays, W. M., "Heat Transfer to a Turbulent Boundary Layer with Varying Free-Stream Velocity and Varying Surface Temperature, An Experimental Study," *International Journal of Heat and Mass Transfer*, Vol. 8, 1965, pp. 1187–1202.

[6] Back, L. H., Massier, P. F., and Cuffel, R. F., "Some Observations on Reduction of Turbulent Boundary-Layer Heat Transfer in Nozzles," *AIAA Journal*, Vol. 4, No. 12, Dec. 1966, pp. 2226–2229.

[7] Kline, S. J., "Observed Structure Features in Turbulent and Transitional Boundary Layers," *Fluid Mechanics of Internal Flow*, edited by G. Sovran, Elsevier, Amsterdam, 1967.

[8] Back, L. H. and Seban, R. A., "Flow and Heat Transfer in a Turbulent Boundary Layer with Large Acceleration Parameter," *Proceedings of the Heat Transfer Fluid Mechanics Institute*, Stanford Univ. Press, 1967, pp. 410–426.

[9] Patel, V. C. and Head, M. R., "Reversion of Turbulent to Laminar Flow," *Journal of Fluid Mechanics*, Vol. 34, Pt. 2, Nov. 1968, pp. 371–392.

[10] Back, L. H., Cuffel, R. F., and Massier, P. F., "Laminarization of a Turbulent Boundary Layer in Nozzle Flow—Boundary Layer and Heat Transfer Measurements with Wall Cooling," *Transactions of the ASME: Journal of Heat Transfer*, to be published.

[11] Levy, S., "Effect of Large Temperature Changes (Including Viscous Heating) Upon Laminar Boundary Layers With Variable Free-Stream Velocity," *Journal of the Aeronautical Sciences*, Vol. 21, No. 7, July 1954, pp. 459–474.

[12] Cohen, C. B. and Reshotko, E., "Similar Solutions for the Compressible Laminar Boundary Layer With Heat Transfer and Pressure Gradient," R-1293, 1956, NACA.

[13] Kemp, N. H., Rose, P. H., and Detra, R. W., "Laminar Heat Transfer Around Blunt Bodies in Dissociated Air," *Journal of the Aerospace Sciences*, Vol. 26, No. 7, July 1959, pp. 421–430.

[14] Beckwith, I. E. and Cohen, N. B., "Application of Similar Solutions to Calculation of Laminar Heat Transfer on Bodies With Yaw and Large Pressure Gradient in High-Speed Flow," TN-D-625, 1961, NASA.

[15] Gross, J. F. and Dewey, C. F., "Similar Solutions of the Laminar Boundary-Layer Equations With Variable Fluid Properties," *Fluid Dynamic Transactions*, Vol. II, edited by W. Fizdon, Pergamon Press, New York, 1965.

[16] Dewey, C. F. and Gross, J. F., "Exact Similar Solutions of the Laminar Boundary-Layer Equations," *Advances in Heat Transfer*, Vol. 4, edited by J. P. Hartnett and T. F. Irvine Jr., Academic Press, New York, 1967, pp. 317–446.

[17] Coles, D., "The Laminar Boundary Layer Near a Sonic Throat," *Proceedings of the Heat Transfer and Fluid Mechanics Institute*, Stanford University Press, 1957, pp. 119–137.

[18] Schlichting, H., *Boundary Layer Theory*, 6th ed., McGraw-Hill, New York, 1968.

[19] Hayes, W. F. and Probstein, R. J., *Hypersonic Flow Theory*, Academic Press, New York, 1959.

[20] Back, L. H., "Flow and Heat Transfer in Laminar Boundary Layers with Swirl," *AIAA Journal*, Vol. 7, No. 9, Sept. 1969, pp. 1781–1789.

[21] Radbill, J. R., "Application of Quasilinearization to Boundary-Layer Equations," *AIAA Journal*, Vol. 2, No. 10, Oct. 1964, pp. 1860–1862.

[22] Libby, P. A. and Chen, K. K., "Remarks on Quasilinearization Applied in Boundary-Layer Calculations," *AIAA Journal*, Vol. 4, No. 5, May 1966, pp. 937–939.

[23] Libby, P. A., "Heat and Mass Transfer at a General Three-Dimensional Stagnation Point," *AIAA Journal*, Vol. 5, No. 3, March 1967, pp. 507–517.

[24] Libby, P. A. and Liu, T. M., "Some Similar Laminar Flows Obtained by Quasilinearization," *AIAA Journal*, Vol. 6, No. 8, Aug. 1968, pp. 1541–1548.

[25] Back, L. H., "Effects of Severe Surface Cooling and Heating on the Structure of Low-Speed, Laminar Boundary-Layer Gas Flows with Constant Free-Stream Velocity," TR 32-1301, 1968, Jet Propulsion Lab., Pasadena, Calif.

[26] Howarth, L., *Modern Developments in Fluid Dynamics—High Speed Flow*, Oxford University Press, London, 1953.

[27] Eckert, E. R. G., "Engineering Relations for Heat Transfer and Friction in High-Velocity Laminar and Turbulent Boundary-Layer Flow Over Surfaces With Constant Pressure and Temperature," *Transactions of the ASME*, Vol. 78, 1956, pp. 1273–1283.

[28] Fay, J. A. and Riddell, F. R., "Theory of Stagnation-Point Heat Transfer in Dissociated Air," *Journal of the Aerospace Sciences*, Vol. 25, No. 2, Feb. 1958, pp. 73–85.

[29] Bade, W. L., "Stagnation-Point Heat Transfer in a High Temperature Inert Gas," *The Physics of Fluids*, Vol. 5, No. 2, Feb. 1962, pp. 150–154.